THE JOURNAL OF PHYSICAL CHEMISTRY B

Article

pubs.acs.org/JPCB

A Molecular Dynamics Examination on Mutation-Induced Catalase Activity in Coral Allene Oxide Synthase

Phil De Luna, Eric A. C. Bushnell, and James W. Gauld*

Department of Chemistry and Biochemistry, University of Windsor, Windsor, Ontario N9B 3P4, Canada

Supporting Information

ABSTRACT: Coral allene oxide synthase (cAOS) catalyzes the formation of allene oxides from fatty acid hydroperoxides. Interestingly, its active site differs from that of catalase by only a single residue yet is incapable of catalase activity. That is, it is unable to catalyze the decomposition of hydrogen peroxide to molecular oxygen and water. However, the single active-site mutation T66V allows cAOS to exhibit catalase activity. We have performed a series of molecular dynamics (MD) simulations in order to gain insights into the differences in substrate (8*R*-hydroperoxyeicosatetraenoic) and H_2O_2 active site binding between wild-type cAOS and the T66V mutant cAOS. It is observed that in wild-type cAOS the active site Thr66 residue consistently forms a strong hydrogen-bonding interaction with H_2O_2 (catalase substrate) and, importantly, with the aid of His67 helps to pull H_2O_2 away from the heme Fe center. In contrast, in the T66V-cAOS mutant the H_2O_2 is much closer to the heme's Fe center and now forms a consistent Fe···O_2H_2 interaction. In addition, the His67···H_2O_2 distance shortens considerably, increasing the likelihood of a Cpd I intermediate and hence exhibiting catalase activity.

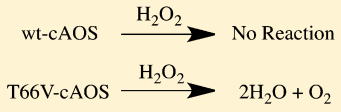

INTRODUCTION

Coral allene oxide synthase (cAOS) is a heme enzyme that was first discovered in the marine invertebrate *Plexaura homomalla* as a fusion protein with 8*R*-lipoxygenase.[1] Importantly, it catalyzes a key step in the formation of the prostanoid clavulone I from arachidonic acid: the oxidation of 8*R*-hydroperoxyeicosatetraenoic (8*R*-HPETE) into a reactive allene oxide (Scheme 1).[2−4] Notably, clavulone I has been shown to display antiviral, anticancer, and antileukemic activity.[5−7] Hence, there is increasing interest in understanding the chemistry and mechanism of this remarkable enzyme.

cAOS shows structural homology with that of catalase, a crucial enzyme that catalyzes the decomposition of H_2O_2 to H_2O and O_2.[9] Indeed, the active site of wild-type (WT) cAOS essentially differs from catalase by only one active site residue. Specifically, the former contains a threonyl (Thr66) while in catalase this is replaced by a valinyl (Val74).[9,10] Notably, several studies have examined the roles of active site residues surrounding the heme groups in cAOS and catalase.[9−13] For instance, Gao et al.[11] examined experimentally the effect on the rate of reaction of mutating a conserved asparagine residue. In cAOS the rate of reaction was significantly decreased to just 0.8−4.0% of WT-cAOS but, importantly, allene oxide was still produced by all mutants. For catalase the rate of reaction was only decreased by 20%. However, the distal heme Asn was deemed to be not essential in either catalase or cAOS; rather, its presence in these enzymes relates to a role in optimizing catalysis.[11]

It is known that the iron centers proximal ligand in heme enzymes can affect the catalytic reactions.[14] In both catalase and cAOS the Fe center of the heme is ligated to the protein via a proximal tyrosyl ligand. However, Wu et al.[13] have shown through experimental EPR studies that cAOS homolytically cleaves the O−O bond in its native substrate (8*R*-HPETE) while in catalases the O−O bond in the H_2O_2 substrate is cleaved heterolytically. In fact, despite sharing similar heme-binding environments, e.g., tyrosyl−iron ligation, conserved catalytic residues, and a catalase active-site fold, cAOS shows no catalase activity.[9,10,15] It has been proposed[10] that in WT-cAOS the Thr66 residue hydrogen bonds with the distal His67, causing a rotation of the histidyl's imidazole ring. The latter would presumably be important in a catalase-like shuttling of the proton from the proximal oxygen of H_2O_2 to the distal oxygen allowing for the formation of water and the oxo-ferryl species. Hence, formation of the key catalase mechanism intermediate oxo-ferryl compound I (Cpd I) is inhibited. It is also noted that to date catalases have not generally been recognized as being directly involved in the synthesis of biomolecules, in contrast with the direct role of cAOS in allene oxide formation.[9,10,16]

Experimentally, it has been demonstrated that the mutation of Thr66 in cAOS to a valinyl (T66V-cAOS) induces catalase activity coupled with a decrease in rate of native cAOS activity.[10] Importantly, it was observed that T66V-cAOS is able to form the Cpd I species, a key intermediate in the catalase mechanism.[10] Thus, it has been suggested that substitution of Thr66 by valinyl eliminates its hydrogen-bonding interaction with His67, freeing the histidyl and allowing for catalase activity in the T66V mutant cAOS.[10] Unfortunately, to date, there has been no experimentally derived NMR or X-ray structure of WT-cAOS or T66V-cAOS with 8*R*-HPETE or H_2O_2 bound within their active sites.

Received: August 24, 2013
Revised: October 26, 2013
Published: October 28, 2013

   dx.doi.org/10.1021/jp408486n | *J. Phys. Chem. B* 2013, 117, 14635−14641

Scheme 1. Catalytic Mechanism of cAOS for the Formation of Allene Oxide from 8*R*-HPETE[8]

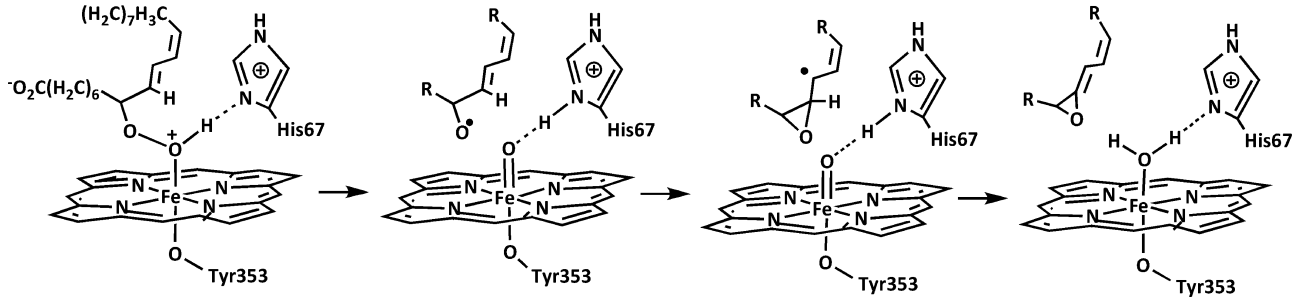

In all enzyme-mediated reactions the formation of the enzyme−substrate complex (i.e., Michaelis complex) is an essential component. Computational methods have gained prominence in the study of enzyme−substrate interactions.[17] In particular, molecular dynamics (MD) methods have been previously successfully applied to study enzyme−substrate binding, effects of mutagenesis, and conformational changes.[18−21] In this present study, we have utilized MD simulations to investigate the binding interactions and enzyme−substrate complexes of WT-cAOS and T66V-cAOS with 8*R*-HPETE (substrate of native cAOS) and H_2O_2 (substrate of catalase). In addition, we have also examined the importance of the catalytic histidyl residue His67 in forming a hydrogen-bonding network with Thr66 and its potential implications for inhibition of catalase activity.

COMPUTATIONAL METHODS

The Molecular Operating Environment (MOE) software was used for model preparation, energy minimizations, and assessment of the generated trajectories.[22] MD simulations were performed using the NAMD program.[23,24]

All models were prepared from the crystal structure obtained by Oldham et al. (PDB ID 1U5U).[1] Initially, all crystallographic waters and counterions were deleted. Furthermore, the C-terminal domain was deleted to reduce computational costs. In particular, it has been shown that the catalytic activity of the N-terminal cAOS domain remains active upon deletion of the C-terminal domain.[12] The protons not present within crystal structure were then added using the default method within MOE. In total, 11 models were generated, a summary of which is listed in Table 1. In particular, models were generated in which the WT-cAOS and T66V-cAOS were prepared with no substrate bound to heme where the iron was modeled as Fe(III) to test model consistency. Models (complexes) were then generated with either the 8*R*-HPETE substrate or H_2O_2 within the active site to study difference in substrate binding to the Fe(III)-heme center. In the case of 8*R*-HPETE the substrate was placed within the active site using a docking simulation. The London dG scoring function was used to estimate the binding free energies of each enzyme−substrate complex, and the geometries for the most favorable 100 docked substrates were then optimized with the PFROSST force field, i.e., the AMBER force field with added parameters for small biomolecules such as heme with the protein fixed and rescored.[22,25] The resulting top scoring configuration was then completely minimized (i.e., substrate and protein) using the PFROSST force field until the root-mean-square gradient of the total energy was calculated to be below 0.05 kcal au^{-1}. This minimized complex was then used for all subsequent MD simulations.

Table 1. Summary of the Enzyme−Substrate Complexes Considered in This Study[a]

	substrate bound WT-cAOS				substrate bound T66V-cAOS		
			H_2O_2				H_2O_2
model	none	8*R*-HPETE	H-bond to H67	H-bond to T66	none	8*R*-HPETE	H-bond to H67
1	×						
2		×					
3		×*					
4			×				
5			×*				
6				×			
7					×		
8						×	
9						×*	
10							×
11							×*

[a]* indicates those in which the imidazole of H67 was rotated as suggested in ref 6.

For the models that contained WT-cAOS with H_2O_2 the long-chain fatty acid chain of 8*R*-HPETE was deleted and replaced with a proton. Furthermore, the initial orientation of H_2O_2 was varied such that it was hydrogen bonded (H-bonded) to either Thr66 or His67. Finally, each enzyme−substrate combination was modeled with a rotated His67 to investigate its effect on substrate binding. It is noted that prior to each MD simulation each of the 11 models was minimized with the PFROSST force field. A schematic representation of each model is provided in Figure S1 in the Supporting Information.

For each of the 11 complexes, the addition of water molecules to mimic a solvated environment was done. In particular, a 6 Å droplet modeled with the TIP3P water model was used to solvate a set region around the active site.[26] The geometry of each enzyme−substrate complex after solvation was then minimized with the PFROSST force field until the root-mean-square gradient of the total energy was below 0.05 kcal mol^{-1} $Å^{-1}$. After minimization, all residues and water molecules beyond the second environmental shell surrounding the heme center were fixed in order to reduce computational costs, but all atoms within the shell were free to move. It should be noted that the long-range electrostatic interactions of the bulk enzyme were still retained despite the geometries being fixed.

Such a protocol has been successfully used in the investigation of the binding of substrate in the active site of UROD and ThrRS.[19] Thus, we feel it is suitable in the present

dx.doi.org/10.1021/jp408486n | J. Phys. Chem. B 2013, 117, 14635−14641

investigation into the binding of 8*R*-HPETE in cAOS. Furthermore, as stated by Leach[27] the use of such an approach is suitable when investigating key aspects of a system such as the active site of an enzyme. However, we have performed additional simulation of model **2** where the complete protein was free to move. Notably, we did not observe any major changes of the active site that would suggest that a protocol of fixing the environment is unsuitable. In particular, it was found that during the simulation of the freed model the active-site interactions observed in the "fixed" MD simulation were consistent. For instance, the distal peroxy oxygen remained in close proximity to the Fe center while the peroxy hydrogen formed a H-bonding interaction with Thr66. Furthermore, the conformation of the heme was found to be consistent between the free and fixed simulations.

As noted above, the MD simulations were performed using the NAMD program which utilizes a velocity Verlet integration method to obtain the trajectories.[28] The PFROSST force field was used for all simulations. A damping functional factor was used to allow the electrostatic and van der Waals potentials to decay smoothly from 8 and 10 Å. Prior to the production runs, annealing of the system from 200 to 300 K over a 0.25 ns period was performed after which 9.75 ns production runs were performed with a time step of 2 fs. It is noted that during the production runs Langevin dynamics were used with the temperature held constant as per the NAMD algorithm.[23,24] Once finished, the MD simulations were imported into MOE with the trajectories clustered into five groups based on the rmsds of Thr66 (or Val66), His67 and heme. The average structure was obtained from the most populated cluster and then used for geometric analysis and comparison to other models.

RESULTS AND DISCUSSION

Holoenzymes. Initial studies examined the consistency of the active sites themselves of the WT- and T66V-cAOS holoenzymes (i.e., complexes **1** and **7**, respectively; see Table 1). Specifically, since the heme is the cofactor responsible for substrate binding its rmsds ($rmsd_{heme}$), with respect to the starting structure of the MD simulation (see Computational Methods), was considered. The average $rmsd_{heme}$'s are given in Table 2 while a plot of $rmsd_{heme}$'s (for all complexes) versus time is given in Figure S2 in the Supporting Information.

Over the course of the MD simulations it is noted that the heme maintained its planarity in both WT-cAOS (**1**) and T66V-cAOS (**7**), as was in fact the case for most complexes investigated. For both WT-cAOS and T66V-cAOS the average $rmsd_{heme}$ values obtained are 0.496 and 0.305, respectively. In fact, for all models the average $rmsd_{heme}$'s lie in the range 0.26–0.68 Å, indicating that regardless of the complex the position of the heme remains reasonably consistent with regard to the respective initial MD structure. It is noted that the largest change in heme position occurred during the initial phase of the simulations during which the temperature was increasing (see Computational Methods).

8*R*-HPETE Binding. The bindings of the long-chain fatty acid substrate 8*R*-HPETE in both the WT-cAOS and T66V-cAOS enzymes, for the two possible orientations of the imidazole of the active site histidyl His67 in each, were then examined; i.e., complexes **2**, **3**, **8**, and **9** were examined (see Table 1).

For each enzyme···8*R*-HPETE complex, an average structure was obtained via a cluster analysis of the corresponding MD simulation. From those complexes involving WT-cAOS, i.e., **2** and **3**, it was observed that regardless of orientation of His67 the native substrate 8*R*-HPETE (HO_2R) formed a weak interaction with the Fe center via an oxygen of its peroxide moiety (Figure 1a). The average $Fe_{heme}\cdots(H)O_2R$ and Thr66-O(H)···HO_2R distances are given in Table 3.

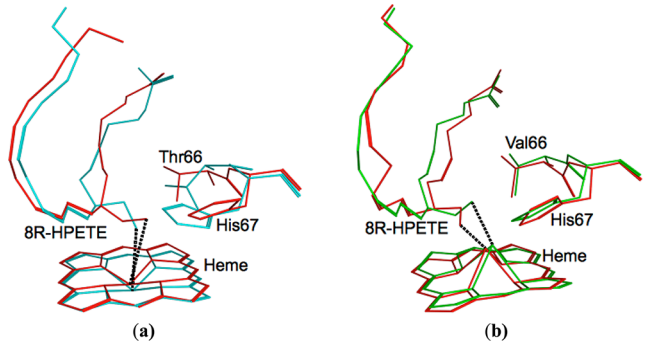

Figure 1. Overlays of the active site heme, His67, Thr66 (or Val66), and bound native substrate 8*R*-HPETE obtained from the MD simulations of (a) complex **2** (light blue) and **3** with (red) His67 rotated and (b) complex **8** without (green) and **9** with (red) His67 rotated. Note that the heme cofactor substituents and all hydrogens have been removed for clarity.

Table 2. Average Rmsds ($rmsd_{heme}$) of the Heme from Initial Minimized Structure for the Various Models over the 10 ns MD Simulation

model	description of initial complex	$rmsd_{heme}$ (Å)
1	WT-cAOS	0.496
2	WT-cAOS, 8*R*-HPETE bound	0.375
3	WT-cAOS, 8*R*-HPETE bound, rotated His67	0.262
4	WT-cAOS, H_2O_2 bound, H-bond to His67	0.682
5	WT-cAOS, H_2O_2 bound, rotated His67	0.483
6	WT-cAOS, H_2O_2 bound, H-bond to Thr66	0.501
7	T66V-cAOS	0.305
8	T66V-cAOS, 8*R*-HPETE bound	0.390
9	T66V-cAOS, 8*R*-HPETE bound, rotated His67	0.401
10	T66V-cAOS, H_2O_2 bound	0.287
11	T66V-cAOS, H_2O_2 bound, rotated His67	0.305

Table 3. Average $r(Fe_{heme}\cdots(H)O_2R)$, r(Thr66—O(H)···HO_2R), and r(His67—Nδ···HO_2R) Distances (Å) for Complexes 2, 3, 8, and 9

complex	av $r(Fe_{heme}\cdots(H)O_2R)$	av r(Thr66—O(H)···HO_2R)	av r(His67—Nδ···HO_2R)
2	3.154	3.280	2.009
3	3.337	1.789	NA
8	2.398	NA	3.695
9	2.366	NA	NA

In particular, it is observed that for the WT-cAOS complex **2** in which the His67 residue is not rotated the average $r(Fe_{heme}\cdots(H)O_2R)$ and r(Thr66-O(H)···HO_2R) distances are 3.154 and 3.281 Å, respectively. It should be noted that over the course of the MD simulation the substrate's peroxide moiety alternated between acting as a hydrogen bond donor to either the hydroxyl moiety of Thr66 or the deprotonated nitrogen on the imidazole of His67. However, the interaction with the

dx.doi.org/10.1021/jp408486n | J. Phys. Chem. B 2013, 117, 14635–14641

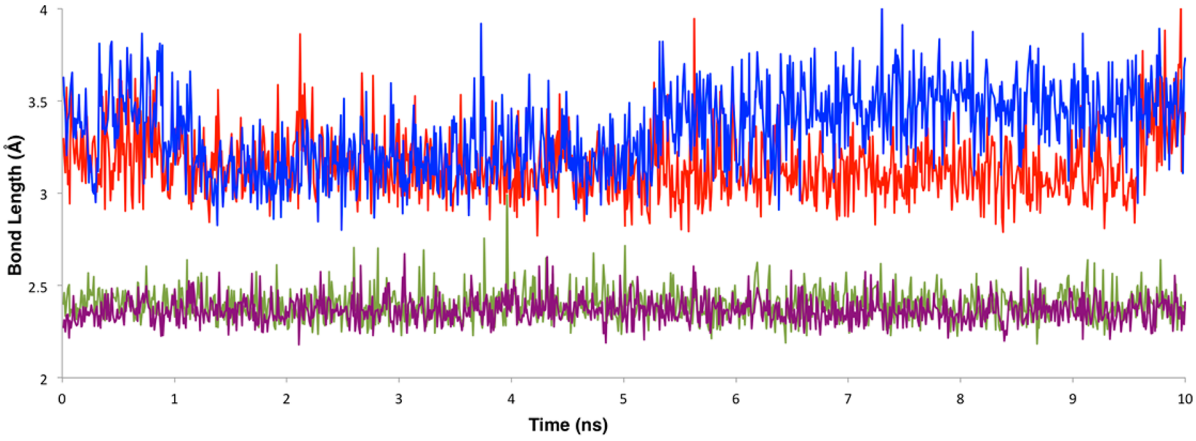

Figure 2. Plot of $Fe_{heme}\cdots(H)O_2R$ distances with respect to time (ns) for the MD simulations of complexes **2** (red), **3** (blue), **8** (green), and **9** (purple).

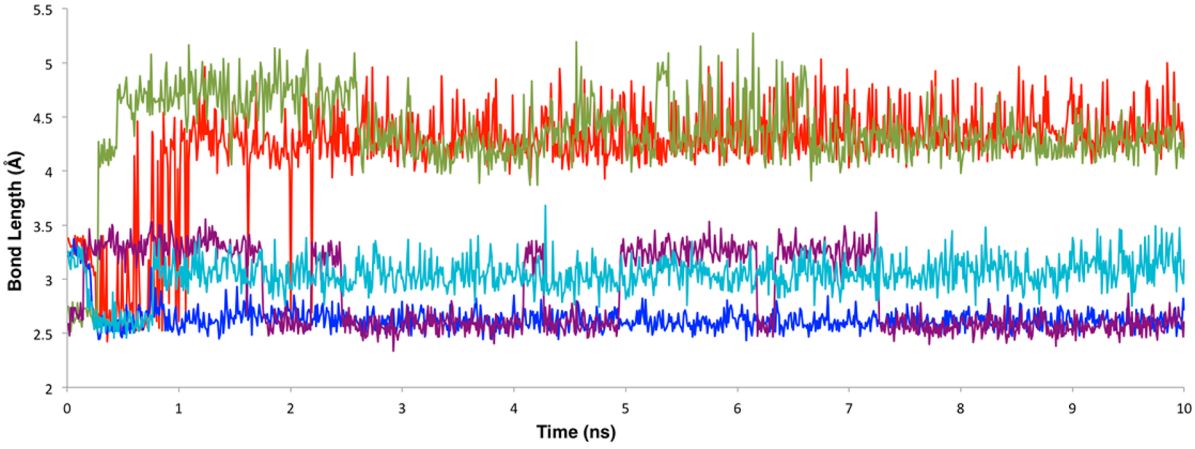

Figure 3. Plot of the $Fe_{heme}\cdots O_2H_2$ distances with respect to time for the 10 ns MD simulations of complexes **4** (red), **5** (dark blue), **6** (green), **10** (purple), and **11** (light blue).

imidazole of His67 was generally stronger. Indeed, r(His67—N$\delta\cdots HO_2R$) was found to be 2.01 Å (Table 3).

This supports our earlier work[8] wherein His67 was proposed to act as a general base in the deprotonation of the peroxide moiety during the catalytic transformation of 8*R*-HPETE to allene oxide. In contrast, in the case of the WT-cAOS with a rotated His67 (i.e., complex **3**) the hydrogen-bonding interaction between the substrate's peroxide moiety and the hydroxyl moiety of Thr66 was consistent throughout the 10 ns simulation. Importantly, due to its rotation, the imidazole of His67 was no longer able to hydrogen bond with the substrate's peroxide moiety and in fact moved away from the substrate as seen in Figure 1a. Notably, this results in a much shorter average r(Thr66—O(H)$\cdots HO_2R$) distance of 1.789 Å but at the cost of a larger average $r(Fe_{heme}\cdots(H)O_2R)$ distance of 3.337 Å.

For binding of 8*R*-HPETE in the T66V-cAOS mutant (i.e., complexes **8** and **9**) it was observed that without the presence of Thr66 the substrate shifts away from the heme (Figure 1b). However, with the presently used force field (see Computational Methods), regardless of the orientation of the imidazole of His67, the Fe center which initially lay below the plane of the ring now lies above the plane of the porphyrin ring. That is, while the metal lies equally out of the plane in all simulations in the case of modes **8** and **9** it now lies above the ring rather than below. Upon inspection of the partial charges for the tyrosinate oxygen and distal peroxy oxygen, it was found that the latter had a greater partial negative charge. Thus, it appears the inversion of the Fe is likely due to the greater electrostatic interaction between the iron and peroxy oxygen. Because of this the average $Fe_{heme}\cdots(H)O_2R$ distances in both complexes **8** and **9** are now significantly smaller than that observed in the corresponding WT-cAOS complexes **2** and **3** by 0.756 and 1.004 Å with distances of just 2.398 and 2.366 Å, respectively. This is further illustrated in the graph of $Fe_{heme}\cdots(H)O_2R$ distances versus time (ns) over the course of the entire 10 ns MD simulation for all four WT-cAOS and T66V-cAOS complexes **2**, **3**, **8**, and **9** shown in Figure 2.

As a result, it appears that the enzyme$\cdots$substrate Thr66—O(H)$\cdots HO_2R$ hydrogen-bonding interaction, which is lacking in the T66V mutant, is likely important for moderating the $Fe_{heme}\cdots(H)O_2R$ interaction and proper positioning of the substrate within the active site.

H_2O_2 Binding. As noted in the Introduction, we have chosen to investigate the binding of H_2O_2 to provide insight toward the lack of catalase activity seen in cAOS. Like that shown above for 8*R*-HPETE, the presence of Thr66 affects the binding of H_2O_2. Specifically, for **4** and **6** there appears to be a significant hydrogen-bonding interaction between the hydroxyl moiety of Thr66 and H_2O_2. In addition, there appears to be a strong interaction between H_2O_2 and the backbone carbonyl of Thr66 as well as the imidazole group of His67. Notably, in

dx.doi.org/10.1021/jp408486n | J. Phys. Chem. B 2013, 117, 14635−14641

these simulations the combination of these interactions aids in pulling the ligand away from the Fe center of the heme resulting in an elongation of $r(Fe_{heme}\cdots O_2H_2)$. In particular, for models **4** and **6** during the simulation it was found that while H_2O_2 was initially weakly interacting with the Fe center during the simulation the H_2O_2 moved away considerably from the metal center (Figure 3). As seen in Table 4 the average

Table 4. $Fe_{heme}\cdots O_2H_2$ Distances (in Å) for MD Simulations Run and Average Structures for the Various Models with H_2O_2 Binding

model	av $r(Fe_{heme}\cdots O_2H_2)$	av r(His67—N$\delta\cdots H_2O_2$)	av r(Thr66—O(H)$\cdots H_2O_2$)	av r(Thr66—CO$\cdots H_2O_2$)
4	4.407	2.546	2.980	2.951
5	2.629	NA	1.963	3.824
6	4.356	3.125	2.463	2.591
10	2.864	2.785	NA	2.785
11	3.039	NA	NA	3.318

$r(Fe_{heme}\cdots O_2H_2)$ was 4.407 and 4.356 Å for model **4** and **6**, respectively. In the case of model **4** it was observed that the oxygen that initially ligated the Fe center broke this interaction and formed an H-bonding interaction with the carbonyl of Thr66, the average r(Thr66—CO$\cdots H_2O_2$) distance being 2.951 Å. The other oxygen, however, alternated between acting as a H-bonding donor to Thr66 and His67. It is noted that during the simulation H_2O_2 favored interacting with His67 as evidenced by the average r(Thr66—O(H)$\cdots H_2O_2$) and r(His67—N$\delta\cdots HO_2R$) distances of 2.980 and 2.456 Å.

Similar to **4**, in **6** the oxygen that was initially interacting with the Fe center breaks this interaction whereby the OH group alternated between forming H-bonding interactions to the backbone carbonyl of Thr66 and the imidazole of His67. In particular, the average r(Thr66—CO$\cdots$ H_2O_2) and r(His67—N$\delta\cdots$ H_2O_2) were found to be 2.546 and 2.951 Å, respectively. In both cases the OH of the peroxide is the H-bond donor. The other oxygen on the other hand formed a weak interaction with the hydroxyl group of Thr66. In particular, the average value for r(Thr66—O(H)$\cdots H_2O_2$) was 2.980 Å.

It is noted that models **4** and **6** were generated such that the H_2O_2 was hydrogen bonding with either Thr66 or His67 in order to test whether these differing interactions had an effect on H_2O_2 binding. As seen in Figure 4, for both models H_2O_2 orientated itself to strongly interact with both Thr66 and His67 within the first 1 ns of the simulation. After this point in the simulation it was found that regardless of initial H-bonding the peroxide never ligated the Fe center. Importantly, an active site water takes up the coordination site previously occupied by the weakly interacting H_2O_2. It is noted that for each model His67 was not found to freely rotate under the given system. Notably, it has been proposed[10] that the lack of cAOS' reactivity toward H_2O_2 is due to the Thr66 forming a hydrogen-bonding network with His67, preventing the imidazole group in aiding in Cpd I formation. However, from the present results it was found that the average distance between the oxygen of the hydroxyl moiety Thr66 and the hydrogen from the imidazole ring of His67 was 6.377 and 6.473 Å for complexes **4** and **6**. Thus, to investigate the effect of a rotated His67 on binding, we manually rotated the imidazole of His67 (complex **5**) prior to performing MD production runs. Notably, it was found that similar to models **4** and **6** with rotation we observed a breaking of the initial $Fe_{heme}\cdots O_2H_2$ interaction and the formation of a strong H-bond to the hydroxyl of Thr66.

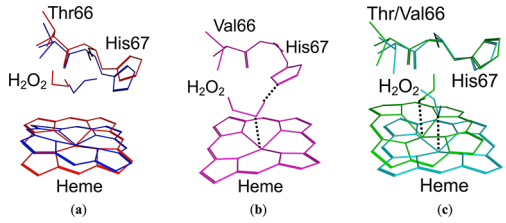

Figure 4. Graphical representations of the average models for H_2O_2 binding. The blue and red models (a) correspond to an overlay of WT-cAOS complex **4** and **6**, the purple model (b) corresponds to **10**, and the teal and green models (c) correspond to an overlay of complexes **5** and **11**. Note that the heme cofactor substituents and all hydrogens have been removed for clarity.

In particular, the average value for r(Thr66—O(H)$\cdots H_2O_2$) was 1.963 Å. However, unlike the other models, the other oxygen that was not initially ligated to the Fe center forms an interaction with the metal center with $r(Fe_{heme}\cdots O_2H_2)$ = 2.63 Å. Importantly, however, due to the rotation of the imidazole of His67 no interaction between H_2O_2 and the imidazole (necessary for catalase activity) is ever observed over the course of the simulation.

In the case of model **10** (i.e., T66V-cAOS), encouraging results were observed. In these models the H_2O_2 seemed to remain interacting with the heme for the entirety of the simulation run. However, if we consider Figure 3 it can be seen that $r(Fe_{heme}\cdots O_2H_2)$ fluctuates between 2.600 and 3.250 Å with an average of 2.864 Å. However, upon closer inspection of the MD trajectories it was found that it is not a single oxygen of the H_2O_2 that ligates to the Fe center. Rather, both oxygens of the peroxide alternate in ligating the Fe center. Notably, if we consider only those complexes where the oxygen used in the determination of the Fe$\cdots$O interaction distance in Figure 3 forms an interaction (i.e., where $r(Fe_{heme}\cdots O_2H_2)$ = ~2.600), in the average complex (Figure 4b) obtained was found such that the proximal oxygen of H_2O_2 also forms a H-bonding interaction with the imidazole of His67. In particular, the average r(His67—N$\delta\cdots$ H_2O_2) was determined to be 2.579 Å. Thus, in order to produce Cpd I the H_2O_2 must bind to the heme in addition to the proximal oxygen forming a hydrogen bond to His67. Hence, the present results suggest that for complex **10** this would occur more readily than seen in **4**, **5**, and **6** enhancing the likely catalase activity, in agreement with experimental evidence.[10,29] To determine if the H_2O_2 remained ligated to the heme for longer than the initial 10 ns, the last structure of the production run for **10** was simulated for an additional 10 ns. Notably, it was observed that H_2O_2 does indeed remain ligated to the Fe center as well as interacting with the imidazole of His67.

For complex **11** (with the imidazole of His67 manually rotated) rather than having a single oxygen ligate the Fe center consistently over the entire simulation the two oxygens of H_2O_2 alternated in ligating the Fe center. However, the average $Fe_{heme}\cdots O_2H_2$ was considerably longer than that seen in model **10**. In particular, the average $r(Fe_{heme}\cdots O_2H_2)$ average distances were measured to be 3.039 and 3.377 Å. However, due to the rotation of the imidazole of His67 no H-bonding interaction was ever observed to occur with H_2O_2. Notably, due to such an interaction it would be expected that catalase activity would be inhibited. Rather, the H_2O_2 alternated between forming H-

dx.doi.org/10.1021/jp408486n | J. Phys. Chem. B 2013, 117, 14635−14641

bonding interactions to the carbonyl of Thr66 or an active site water. It is noted that rotation of His67 did contribute to the elongation of Fe−O distance, but to a greater degree than seen in complex **5**.

CONCLUSIONS

In order to comparatively study the binding of 8*R*-HPETE and H_2O_2 to WT-cAOS and T66V-cAOS, MD simulations were utilized. In particular, the roles of Thr66 and His67 in terms of binding 8*R*-HPETE and H_2O_2 were examined. Listed below are the main findings from this MD study.

(1) In the case of complexes **2** and **3** the substrate (i.e., 8R-HPETE) was found to form an interaction with the heme as expected. However, in those in which Thr66 was mutated (complexes **8** and **9**) it was found that substrate shifted away form the active site. Notably, to maintain the $Fe_{heme}\cdots O_2H_2$ interaction the Fe was found to no longer lie in the plane of the porphyrin ring. Thus, it appears that Thr66 is critical in the proper binding and orientation of the native substrate.

(2) Tosha et al.[10] proposed that the regulation of cAOS catalase activity relies primarily on the distal His67. However, in those complexes in which H_2O_2 was bound within the active site of WT-cAOS (complexes **4** and **6**) the hydrogen-bonding interactions between H_2O_2 and both Thr66 and His67 result in the loss of the $Fe_{heme}\cdots O_2H_2$ interaction. Thus, while a His67$\cdots H_2O_2$ hydrogen-bonding interaction as required for catalase activity is seen, the presence of Thr66 likely inhibits such activity in the native enzyme. Indeed, in complex **10** where Thr66 has been mutated to Val the H_2O_2 remains ligated to the Fe center and forms the necessary hydrogen-bonding interaction with His67. Thus, it appears that catalase activity would likely be exhibited under such conditions.

(3) It is observed that the hydrogen bonding between the substrate's peroxide, for 8*R*-HPETE or H_2O_2, and imidazole of His67 was lost upon rotation of the imidazole of His67. Importantly, in the case of complex **11** this would likely lead to the loss of catalase activity for the T66V mutant.

Hence, from the MD simulations performed it appears that there are two main factors which drastically effect substrate binding, and thus may lead to lack of catalase activity in cAOS: (i) the orientation of the His67 imidazole ring and (ii) the ability for Thr66 to hydrogen bond to H_2O_2.

ASSOCIATED CONTENT

Supporting Information

Schematic representations of the active-site residues for all molecular dynamics simulations performed and heme rmsds with respect to time for the 10 ns MD simulations of complexes **1** through **11**. This material is available free of charge via the Internet at http://pubs.acs.org.

AUTHOR INFORMATION

Corresponding Author

*E-mail: gauld@uwindsor.ca.

Notes

The authors declare no competing financial interest.

ACKNOWLEDGMENTS

We thank the Natural Sciences and Engineering Research Council of Canada (NSERC), Canada Foundation for Innovation (CFI), the Ontario Innovation Trust (OIT), and SHARCNET for additional computational resources and graduate scholarships (E.A.C.B.). E.A.C.B. also thanks NSERC for a PGS3D Scholarship.

REFERENCES

(1) Oldham, M. L.; Brash, A. R.; Newcomer, M. E. Insights From The X-Ray Crystal Structure Of Coral 8R-Lipoxygenase. *J. Biol. Chem.* **2005**, *280*, 39545−39552.

(2) Koljak, R.; Boutaud, O.; Shieh, B. H.; Samel, N.; Brash, A. R. Identification Of A Naturally Occurring Peroxidase-Lipoxygenase Fusion Protein. *Science* **1997**, *277*, 1994−1996.

(3) Tijet, N.; Brash, A. R. Allene Oxide Synthases And Allene Oxides. *Prostaglandins Other Lipid Mediators* **2002**, *68*, 423−431.

(4) Gilbert, N. C.; Niebuhr, M.; Tsuruta, H.; Bordelon, T.; Ridderbusch, O.; Dassey, A.; Brash, A. R.; Bartlett, S. G.; Newcomer, M. E. A Covalent Linker Allows for Membrane Targeting of an Oxylipin Biosynthetic Complex. *Biochemistry* **2008**, *47*, 10665−10676.

(5) Huang, Y. C.; Guh, J. H.; Shen, Y. C.; Teng, C. M. Investigation Of Anticancer Mechanism Of Clavulone II, A Coral Cyclopentenone Prostaglandin Analog, In Human Acute Promyelocytic Leukemia. *J. Biomed. Sci.* **2005**, *12*, 335−345.

(6) Bader, T.; Yamada, Y.; Ankel, H. Antiviral Activity Of The Prostanoid Clavulone II Against Vesicular Stomatitis Virus. *Antiviral research* **1991**, *16*, 341−355.

(7) Honda, A.; Yamamoto, Y.; Mori, Y.; Yamada, Y.; Kikuchi, H. Antileukemic Effect Of Coral-Prostanoids Clavulones From The Stolonifer Clavularia Viridis On Human Myeloid Leukemia (HL-60) Cells. *Biochem. Biophys. Res. Commun.* **1985**, *130*, 515−523.

(8) Bushnell, E. A. C.; Gherib, R.; Gauld, J. W. Insights into the Catalytic Mechanism of Coral Allene Oxide Synthase: A Dispersion Corrected Density Functional Theory Study. *J. Phys. Chem. B* **2013**, *117*, 6701−6710.

(9) Oldham, M. L.; Brash, A. R.; Newcomer, M. E. The Structure Of Coral Allene Oxide Synthase Reveals A Catalase Adapted For Metabolism Of A Fatty Acid Hydroperoxide. *Proc. Natl. Acad. Sci. U.S.A.* **2005**, *102*, 297−302.

(10) Tosha, T.; Uchida, T.; Brash, A. R.; Kitagawa, T. On the Relationship of Coral Allene Oxide Synthase to Catalase. *J. Biol. Chem.* **2006**, *281*, 12610−12617.

(11) Gao, B.; Boeglin, W. E.; Brash, A. R. Role Of The Conserved Distal Heme Asparagine Of Coral Allene Oxide Synthase (Asn137) And Human Catalase (Asn148): Mutations Affect The Rate But Not The Essential Chemistry Of The Enzymatic Transformations. *Arch. Biochem. Biophys.* **2008**, *477*, 285−290.

(12) Boutaud, O.; Brash, A. R. Purification and Catalytic Activities of the Two Domains of the Allene Oxide Synthase-Lipoxygenase Fusion Protein of the CoralPlexaura homomalla. *J. Biol. Chem.* **1999**, *274*, 33764−33770.

(13) Wu, F.; Katsir, L. J.; Seavy, M.; Gaffney, B. J. Role Of Radical Formation At Tyrosine 193 In The Allene Oxide Synthase Domain Of A Lipoxygenase-AOS Fusion Protein From Coral. *Biochemistry* **2003**, *42*, 6871−6880.

(14) Poulos, T. L. The Role Of The Proximal Ligand In Heme Enzymes. *J. Biol. Inorg. Chem.* **1996**, *1*, 356−359.

(15) Abraham, B. D.; Sono, M.; Boutaud, O.; Shriner, A.; Dawson, J. H.; Brash, A. R.; Gaffney, B. J. Characterization Of The Coral Allene Oxide Synthase Active Site With UV-Visible Absorption, Magnetic Circular Dichroism, And Electron Paramagnetic Resonance Spectroscopy: Evidence For Tyrosinate Ligation To The Ferric Enzyme Heme Iron. *Biochemistry* **2001**, *40*, 2251−2259.

(16) Chelikani, P.; Fita, I.; Loewen, P. Diversity Of Structures And Properties Among Catalases. *Cell. Mol. Life Sci.* **2004**, *61*, 192−208.

(17) Llano, J.; Gauld, J. W. Mechanistics of Enzyme Catalysis: From Small to Large Active-Site Models. In *Quantum Biochemistry: Electronic Structure and Biological Activity*; Matta, C. F., Ed.; Wiley-VCH: Weinheim, Germany, 2010.

(18) Karplus, M.; McCammon, J. A. Molecular Dynamics Simulations Of Biomolecules. *Nat. Struct. Mol. Biol.* **2002**, *9*, 646−652.

(19) (a) Bushnell, E. A. C.; Huang, W.; Llano, J.; Gauld, J. W. Molecular Dynamics Investigation into Substrate Binding and Identity of the Catalytic Base in the Mechanism of Threonyl-tRNA Synthetase. *J. Phys. Chem B* **2012**, *116*, 5205−5212. (b) Bushnell, E. A. C.; Erdtman, E.; Llano, J.; Eriksson, L. A.; Gauld, J. W. The First Branching Point in Porphyrin Biosynthesis: A Systematic Docking, Molecular Dynamics and Quantum Mechanical/Molecular Mechanical Study of Substrate Binding and Mechanism of Uroporphyrinogen-III Decarboxylase. *J. Comput. Chem.* **2011**, *32*, 822.
(20) Amara, P.; Andreoletti, P.; Jouve, H. M.; Field, M. J. Ligand Diffusion In The Catalase From Proteus Mirabilis: A Molecular Dynamics Study. *Protein Sci.* **2001**, *10*, 1927−1935.
(21) Banci, L. Molecular Dynamics Simulations Of Metalloproteins. *Curr. Opin. Chem. Biol.* **2003**, *7*, 143−149.
(22) *Molecular Operating Environment*, 2012.10 ed.; Chemical Computing Group Inc.: Montreal, Quebec, Canada, 2012.
(23) Phillips, J. C.; Braun, R.; Wang, W.; Gumbart, J.; Tajkhorshid, E.; Villa, E.; Chipot, C.; Skeel, R. D.; Kale, L.; Schulten, K. Scalable molecular dynamics with NAMD. *J. Comput. Chem.* **2005**, *26*, 1781−1802.
(24) Bhandarkar, M.; Bhatele, A.; Bohm, E.; Brunner, R.; Buelens, F.; Chipot, C.; Dalke, A.; Dixit, S.; Fiorin, G.; Freddolino, P.; et al. *NAMD User's Guide, Version 2.7 b1*; Theoretical Biophysics Group, Beckman Institute, University of Illinois: Urbana, IL, 2009.
(25) Wang, J.; Cieplak, P.; Kollman, P. J. How Well Does a Restrained Electrostatic Potential (RESP) Model Perform in Calcluating Conformational Energies of Organic and Biological Molecules. *J. Comput. Chem.* **2000**, *21*, 1049−1074.
(26) Jorgensen, W. L.; Chandrasekhar, J.; Madura, J. D.; Impey, R. W.; Klein, M. L. Comparison Of Simple Potential Functions For Simulating Liquid Water. *J. Chem. Phys.* **1983**, *79*, 926.
(27) Leach, A. R. *Molecular Modelling: Principles and Appications*, 2nd ed.; Pearson Education Ltd.: London, 2001.
(28) Allen, M. P.; Tildesley, D. J. *Computer Simulation of Liquids*; Oxford University Press: Oxford, UK, 1989.
(29) Fita, I.; Rossmann, M. G. The Active Center Of Catalase. *J. Mol. Biol.* **1985**, *185*, 21−37.